Observational Study

Medicine®

OPEN

STROBE—A preliminary investigation of IVIM-DWI in cardiac imaging

Shi-Feng Xiang, MB[a], Xue-Qiang Zhang, MM[b,*], Su-Jun Yang, MB[a], Bo Hou, MM[a], Yu-Fang Wang, MB[a], Shuang Huo, MM[c], Xiao-Lei Dong, MB[a], Zhen Yang, MB[a]

Abstract

This study aims to explore the possibility to apply intravoxel incoherent motion-magnetic resonance imaging (IVIM-MRI) in cardiac imaging.

Multi-b-value diffusion-weighted imaging (DWI) sequence scanning was performed on 12 healthy volunteers. A double exponential model was adopted, and the b-value sequence was 0, 20, 60, 80, 120, 200, and 600 second/mm^2. The D-value, D*-value, and f-value of the anterior posterior and lateral walls of the ventricular septum were respectively measured on the short axis section of the heart, the parameters of the myocardium in different blood supply areas in each segment were recorded, and the measured data of these different segments were compared using analysis of variance.

Among these 12 healthy volunteers, the D-value, D*-value, and f-value of these 72 segments were not exactly equal, the D-values of the myocardium in the 5th and 11th segment were lower than those in the 2nd, 3rd, 8th, and 9th segments, and the pairwise differences were statistically significant ($P < .001$). Furthermore, the difference in D-value between the 5th and 11th segments was not statistically significant ($P = 1.000$). The D*-value and f-value of the myocardium in the 5th and 11th segment were higher than those in the 2nd, 3rd, 8th, and 9th segments, and the pairwise differences were statistically significant ($P < .001$). Furthermore, the differences in D*-value and f-value between the 5th and 11th segments was not statistically significant ($P = .214, .787$).

The intravoxel incoherent motion diffusion-weighted imaging (IVIM-DWI) technique can quantitatively reflect the diffusion and blood perfusion status of the myocardium.

Abbreviations: CE-MRI = contrast-enhanced magnetic resonance imaging, DWI = diffusion-weighted imaging, ECG = electrocardiogram, FOV = frequency-coding field of view, IVIM = intravoxel incoherent motion, IVIM-DWI = intravoxel incoherent motion diffusion-weighted imaging, IVIM-MRI = intravoxel incoherent motion-magnetic resonance imaging, NEX = number of excitations, NMR = nuclear magnetic resonance, ROI = region of interest, TE = echo time, TR = repetition time, true FISP = the true fast imaging with steady-state precession.

Keywords: diffusion-weighted imaging, IVIM, magnetic resonance imaging

1. Introduction

Magnetic resonance multi-b-value diffusion-weighted imaging (DWI) is an imaging technology based on the intravoxel incoherent motion (IVIM) theory.[1,2] This technology can noninvasively reflect the diffusion of water molecules and microvascular perfusion in tissues without the use of contrast agents, accordingly avoiding the risk of allergy to contrast agents and gadolinium-related nephrogenic systemic fibrosis.[3] Multi-b-value DWI was first used for brain imaging, and was gradually used for imaging other parts.[4–7] In 2011, Rapacchi et al[8] used the low-b-value DWI sequence for heart scans in healthy volunteers, where the image signal-to-noise ratio and contrast-to-noise ratio could also reach the diagnostic level. However, the application of high-b-value DWI remains difficult. The main reasons are as follows: The distortion of the image is severe. Due to respiratory movement and cardiac pulsation, the displacement of water molecules in the duration of the diffusion gradient leads to a serious loss of signal. The higher the b-value is, the more significant the loss of signal became.[9,10] The quality of the echo planar imaging (EPI) image collected is low, which is mainly characterized by low signal-to-noise ratio.

The integrated slice-by-slice shimming (iShim) sequence is an improvement of the traditional EPI sequence.[11] Compared with the conventional single-shot spin-echo (ss-EPI) sequence, the advantages of iShim-EPI are as follows: it reduces the distortion of the image, in which the B0-Map is scanned before each slice is scanned, and B0-Map signal changes are used to correct the distortion of the EPI images, greatly improving the image distortion problem[12,13]; the corresponding b-value can be reasonably selected according to the requirements of the experiment, improving the accuracy of the D-value, D*-value, and F-value fitting[14,15]; the method of image acquisition is optimized, which allows for the use of a larger number of excitations (NEX), improves the signal-to-noise ratio, and further improves the accuracy of the parameter fitting. The IVIM-DWI technology based on the iShim-EPI sequence can provide more accurate information in cardiac imaging. In the present study, the

Editor: Heye Zhang.

The authors have no conflicts of interest to disclose.

[a] Department of Radiology, [b] President Office, [c] Department of Scientific Research, Handan Central Hospital, Handan, China.

[*] Correspondence: Xue-Qiang Zhang, President Office, Handan Central Hospital, No. 15, Zhonghua South Street, Hanshan District, Handan 056001, China (e-mail: xueqiangzhang_dr@163.com).

Copyright © 2018 the Author(s). Published by Wolters Kluwer Health, Inc. This is an open access article distributed under the terms of the Creative Commons Attribution-Non Commercial-No Derivatives License 4.0 (CCBY-NC-ND), where it is permissible to download and share the work provided it is properly cited. The work cannot be changed in any way or used commercially without permission from the journal.

Medicine (2018) 97:36(e11902)

Received: 22 May 2018 / Accepted: 16 July 2018

http://dx.doi.org/10.1097/MD.0000000000011902

application of multi-b-value DWI sequences in myocardial imaging was preliminarily explored, and the possibility of its clinical application in cardiac imaging was discussed, in order to provide reference for related studies.

2. Materials and methods

2.1. General information

A total of 12 healthy volunteers were enrolled into the present study. Among these subjects, 7 subjects were male and 5 subjects were female. The age of these subjects ranged within 23 to 53 years old, with an average age of 35.7 years old. The heart rates of these subjects were within 50 to 82 bpm, and their cardiac rhythms were roughly normal. Inclusion criteria: subjects without a history of cerebrovascular and pulmonary diseases, and the absence of cardiac muscle injury and fibrosis in these subjects were confirmed by contrast-enhanced magnetic resonance imaging (CE-MRI) examination. Exclusion criteria: patients with serious cardiovascular and cerebrovascular diseases, and other incompatible patients; patients who are unable to undergo a CE-MRI examination (including claustrophobia, or pacemaker or defibrillator in the body). This study was conducted in accordance with the declaration of Helsinki and approved by Ethics Committee of the hospital. All subjects provided a signed informed consent.

2.2. Instruments and scanning modes

A Siemens SKYRA 3.0T MRI scanner was used, which was equipped with a phased array surface coil and electrocardiogram (ECG)-gating technology. The movies of the cross section and coronal plane of the black blood sequence and multisections of the true fast imaging with steady-state precession (true FISP) sequence (4-chamber view and 2-chamber view of the left ventricle, long axis view of the left ventricle passing through the outflow tract of the left ventricle, and continuous 9 to 12 layers of the short axis view from the atrioventricular valve ring to the cardiac apex) were routinely acquired. All patients underwent a delayed enhanced sequence scan of the myocardium and multiple low-b-value DWI sequence scanning of the short axis of the heart. The b-values (a parameter of the diffusion sensitive gradient field) were 0, 20, 60, 100, 150, 200, and 600 second/mm^2, respectively. The scanning parameters were as follows: frequency-coding field of view (FOV) was 306 mm, phase-coding FOV was 75%, repetition time (TR) was 2200 milliseconds, echo time (TE) was 67 milliseconds, the thickness of slice was 8 mm, the gap was 1.5 to 3.5 mm, and the NEX was 8.00. Local shimming and the ECG-gating system were used. Scanning while breath-holding was performed at the end of expiration.

2.3. Image analysis

The data acquired through the IVIM sequence were uploaded to the Syngo. via workstation by 2 senior physicians engaged in cardiovascular imaging diagnoses. The data were analyzed using the corresponding software package. With delayed-enhancement images as the reference, on the DWI (b = 120 second/mm^2) of the basal part and middle part of the short axis view, one region of interest (ROI) in the anterior, posterior and lateral walls of the ventricular septum was selected, respectively, and the pseudocolor images with the D-value, D*-value, and f-value were obtained. The parameters were expressed as mean ± standard deviation.

IVIM-DWI image grading criteria: grade I: the presence of serious deformed artifacts, serious loss of signal of the myocardium found in one or more of the b-value images, and quantitative measurement could not be carried out; grade II: local presence of a small number of artifacts, the myocardium of each b-value image is clear, and the measurement of the ROI is not affected; grade III: no artifact for interference, the myocardium of each b-value image is clear, and the outlines are clear and sharp. In the present study, the images of the 12 patients all met the criteria of grade II or III, and these could be measured.

2.4. Statistical analysis

Measurement data were expressed as mean ± standard deviation (x ± SD). The D-value, D*-value, and f-value of myocardium in different segments of the left ventricle were analyzed using analysis of variance. The data were analyzed using statistical software SPSS 19.0. $P < .05$ was considered statistically significant.

3. Results

Six original b-value DWI images on the short axis view of the left ventricle were acquired from each patient. When the b-value was 0 second/mm^2, the blood flow signals of the heart cavity were hyperintense, and the signals of the myocardium were slightly hyperintense. As the b-value increased, the blood flow signal of the cardiac chambers decreased and gradually became nonsignal, and the signals of the myocardium also gradually decreased. When the b-value was 600 second/mm^2, the signal of the myocardium was low (Fig. 1 A–F), and the pseudocolor images of the D-value (Fig. 2A), D*-value (Fig. 2B), and f-value (Fig. 2C) were obtained. The D-value, D*-value, and f-value of the ROI in each segment of the left ventricle on the IVIM image are presented in Tables 1–3.

Statistical results revealed that the D-value, D*-value, and f-value of the myocardium in each segment of the left ventricle were not exactly equal. Among these, the D-values of the myocardium in the 5th and 11th segment were lower than those in the 2nd, 3rd, 8th, and 9th segments, and the pairwise differences were statistically significant ($P < .001$). However, the difference in D-value between the 5th and 11th segments was not statistically significant ($P = 1.000$). The D*-values and f-values of the myocardium in the 5th and 11th segment were higher than those in 2nd, 3rd, 8th, and 9th segments, and the pairwise differences were statistically significant ($P < .001$). However, the differences in D*-value and f-value between the 5th and 11th segments was not statistically significant ($P = .214$, .787).

4. Discussion

4.1. The basic principle of IVIM

Labeled nuclear magnetic resonance (NMR) cardiac motion image sequences provide an effective way to analyze complex cardiac motion. Currently, the clinic relies mainly on visual observation and manual calibration of doctors for diagnosis, and the workload is large and lacks quantitative and accurate evaluation. Cardiac biventricular segmentation can help doctors obtain clinical indicators such as the quality and volume of the left ventricle and right ventricle. The boundary of the

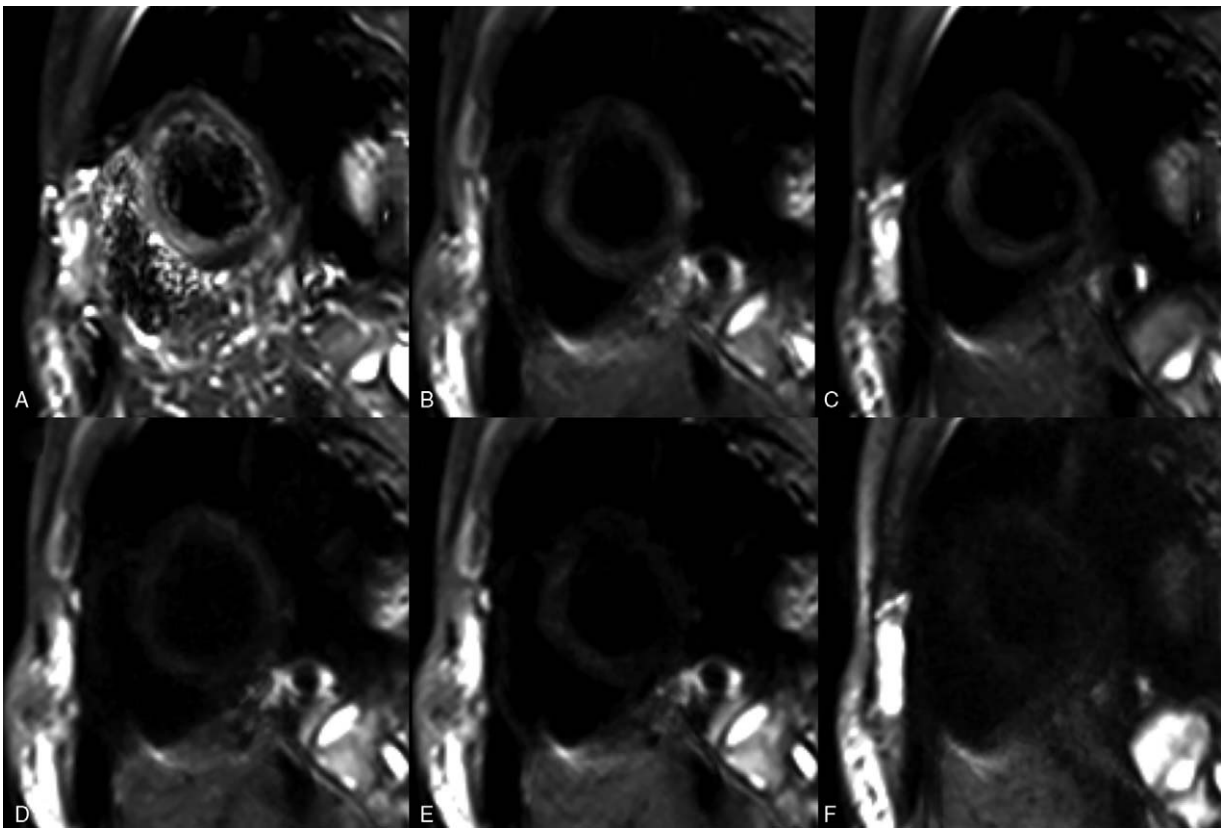

Figure 1. Short axis multi-b-value DWI images of the heart, revealing uniform signals of the myocardium in the left ventricle. No artifacts were found, and the signal of the myocardium decreased with the increase in b-value.

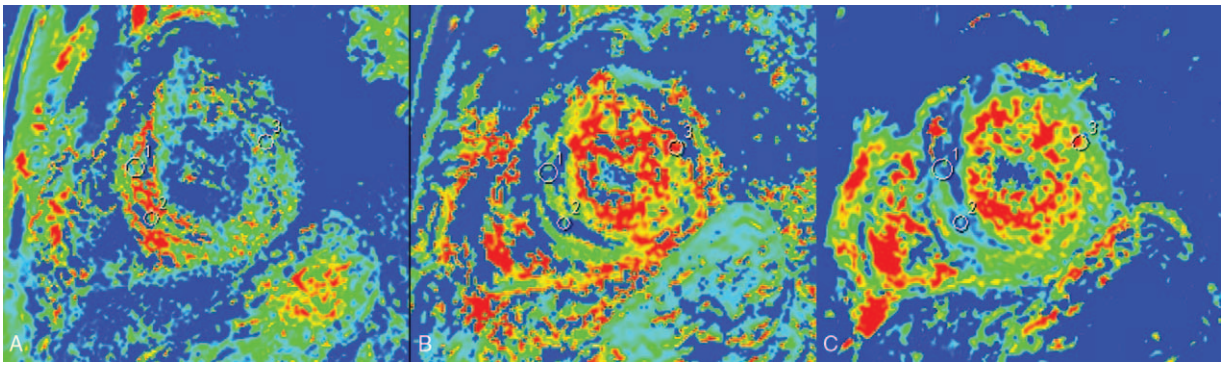

Figure 2. Heart pseudocolor parameters of the anterior septum, lower septum, and lateral wall of the left ventricle were measured. (A) The pseudocolor image corresponding to the D-values. (B) The pseudocolor image corresponding to the D*-values. (C) The pseudocolor image corresponding to the f-values.

Table 1

The D-value of the ROI in each segment of the left ventricle on the IVIM image.

Segment	N	Mean	Std	95% CI	
				Lower limit	Upper limit
2	12	0.0035	0.00031	0.0033	0.0037
3	12	0.0033	0.00039	0.0030	0.0035
5	12	0.0017	0.00023	0.0015	0.0018
8	12	0.0034	0.00025	0.0033	0.0036
9	12	0.0034	0.00022	0.0032	0.0035
11	12	0.0017	0.00026	0.0015	0.0018

CI = confidence interval, IVIM = intravoxel incoherent motion, ROI = region of interest.

Table 2

The D*-value of the ROI in each segment of the left ventricle on the IVIM image.

Segment	N	Mean	Std	95% CI	
				Lower limit	Upper limit
2	12	0.5067	0.0489	0.4756	0.5377
3	12	0.5308	0.0271	0.5136	0.5481
5	12	0.6825	0.0328	0.6617	0.7033
8	12	0.5308	0.0493	0.4995	0.5621
9	12	0.5100	0.0305	0.4907	0.5293
11	12	0.7042	0.0565	0.6683	0.7401

CI = confidence interval, IVIM = intravoxel incoherent motion, ROI = region of interest.

biventricular is divided from the cardiac magnetic resonance image by establishing an automatic and accurate regression model. On this basis, a motion grid energy model is designed to extract and track the intersection of marker lines in cardiac motion image sequences.[16,17] The method can effectively segment the left ventricle, and the measurement of the image parameters has good reproducibility, and can overcome the noise in the cardiac magnetic resonance image and the influence of the surrounding tissue of the heart. It has good accuracy.

DWI is the only imaging method that can observe the microcosmic motion of water molecules in living tissue, and is the most mature and important inspection approach among present functional MRI technologies.[5–7] However, traditional DWI technology does not distinguish the different modes of transportation of water molecules in tissues. Based on the IVIM theory, DWI imaging is performed at multiple b-values in a double exponential model, and the measured values of the corresponding voxels on different b-value images are fitted. Hence, the parameter diagram of the true diffusion coefficient (slow diffusion motion component [D]), pseudo diffusion coefficient (fast diffusion motion component [D*]), and perfusion fraction (f) are acquired, which more accurately reflects the information of blood flow perfusion and water molecular diffusion in the myocardium.[8,9]

4.2. Selecting the b-value

The higher the b-value is, the more sensitive it is to the diffusion movement of water molecules, and the closer it is to the true diffusion movement of water molecules. Its main difficulty in applications to the heart is that the respiratory movement and heart pulsation lead to the distortion of the image, which affects the accuracy of the measurement, causing serious loss of signal.[10–13,18] With the development of MRI software and hardware, and the increase in compatibility of respiratory navigation technology, ECG-gating technology and DWI sequence, this difficulty has been gradually overcome. In the present study, the short axis view DWI image of the heart was used. Six low b-values within 0 to 200 second/mm^2 and one highest b-value of 600 second/mm^2 were chosen. The quality of the scanned images was relatively stable, and the parameter measurement in the ROI was also relatively reliable. The images of the screened 12 healthy volunteers reached grade II or III, no significant loss of signal of the myocardium was observed, and the outline of the myocardium was clear. The repeatability and clinical value of this approach are high in clinical applications. However, its further popularization requires a variety of in-depth studies.

4.3. Preliminary exploration of the characteristics of the D-value, D*-value, and f-value of the myocardium in the left ventricle

The different segments of the left ventricle are supplied with blood by the left coronary artery and circumflex branch of the left coronary artery, and the right coronary artery. Most Chinese people are right coronary artery-dominant type. Therefore, the anterior wall and anterior interventricular septum of the left ventricle are mainly supplied with blood by the anterior descending branch of the left coronary artery; the inferior wall and inferior septum of the left ventricle are mainly supplied with blood by the right coronary artery, and the lateral wall of the left ventricle is mainly supplied with blood by the circumflex branch. The left ventricle is presently studied through the commonly used "17-segment analysis method" in the international community.[19–21] Since the cardiac apex is relatively thin, on short axis DWI images, the anterior and lower wall easily produce slight artifacts, and the parameter values of the DWI images are greatly disturbed. Therefore, these were not included in the measurement indexes in the present study. In the present experiment, the

Table 3

The f-value of the ROI in each segment of the left ventricle on the IVIM image.

Segment	N	Mean	Std	95% CI	
				Lower limit	Upper limit
2	12	0.1983	0.0316	0.1783	0.2184
3	12	0.2158	0.0278	0.1982	0.2335
5	12	0.3608	0.0370	0.3373	0.3844
8	12	0.2183	0.0379	0.1943	0.2424
9	12	0.1942	0.0303	0.1749	0.2134
11	12	0.3650	0.0549	0.3301	0.3999

CI = confidence interval, IVIM = intravoxel incoherent motion, ROI = region of interest.

parameters of the myocardium in the proximal and middle segments of the left ventricle were measured. The 2nd and 8th segments represent the blood supply of the anterior descending branch, the 3rd and 9th segments represent the blood supply of the right coronary artery, and the 5th and 11th segments represent the blood supply of the circumflex branch.[8,22,23]

In the experiment, the D-value, D*-value, and f-value of the myocardium in different segments of the left ventricle were not exactly equal, and the differences between some myocardia were statistically significant. The D-value in myocardium in the 2nd, 8th and 3rd, 9th segments in left ventricle was higher than those in the 5th and 11th segments of the left ventricle. The differences in D-values of the blood supply between the anterior descending branch and circumflex branch, as well as between the right coronary artery and circumflex branch, were statistically significant. However, the difference in the D-value of the blood supply between the anterior descending branch and right coronary artery was not statistically significant. Furthermore, the D*-value and f-value were contrary to the D-value. The D*-value and f-value in the myocardium in the 2nd, 8th and 3rd, 9th segments in the left ventricle were lower than those in the 5th and 11th segments of the left ventricle. The differences in D*-value and f-value in the blood supply between the anterior descending branch and circumflex branch, as well as between the right coronary artery and circumflex branch, were statistically significant. However, the difference in D*-value in the blood supply between the anterior descending branch and right coronary artery was not statistically significant. Thus, the D-value, D*-value, and f-value obtained at multiple low-b-value DWI sequences in the present experiment may be correlated to the blood flow of cardiac perfusion. Studies have revealed that blood flow in the left coronary artery is generally greater than that in the right coronary artery, and blood flow in the left anterior descending branch is the largest, which is only slightly affected by the dominant type. Coronary artery dominant types are diverse in normal populations. However, most Chinese people are right dominant type, in which blood flow in the right coronary artery is often greater than that in the left circumflex branch. In the present experiment, the D-value of the blood supply area in the anterior descending branch and right coronary artery was higher than that of the left circumflex branch, while the D*-value and f-value of the blood supply area in the anterior descending branch and right coronary artery were lower than that of the left circumflex branch. This is similar to the results of other studies. However, the differences in parameters between the anterior descending branch and right coronary artery were not statistically significant. Therefore, this result has a certain value for indicating the different blood supplies and blood flow in the myocardium.

In the present study, a preliminary exploration of the application of the IVIM technique in the myocardium was performed, and parameter values such as the D-value, D*-value, and f-value were compared and analyzed. The results suggest that this has certain significance. However, the sample size was small. Future studies should expand the sample size, improve the imaging technology and improve the quality of the image, and further compare and analyze all segments of the myocardium, in order to investigate the relationship between myocardial perfusion and delayed enhancement. The IVIM scan of the myocardium does not require the use of contrast agents, and can suggest myocardial perfusion and diffusion information. Therefore, this technology would be of great value in the differential diagnosis of myocardial lesions, and its application prospect would very broad.

Author contributions

Conceptualization: Shifeng Xiang, Xueqiang Zhang.
Data curation: Bo Hou, Yufang Wang.
Formal analysis: Shuang Huo, Xiaolei Dong.
Investigation: Sujun Yang.
Methodology: Shuang Huo, Xiaolei Dong.
Resources: Zhen Yang.
Software: Shuang Huo.
Supervision: Xueqiang Zhang.
Writing – original draft: Shifeng Xiang, Xueqiang Zhang.
Writing – review & editing: Shifeng Xiang, Xueqiang Zhang.

References

[1] Le Bihan D, Breton E, Lallemand D, et al. Separation of diffusion and perfusion in intravoxel incoherent motion MR imaging. Radiology 1988;168:497–505.
[2] Clark CA, Le Bihan D. Water diffusion compartmentation and anisotropy at high b values in the human brain. Magn Reson Med 2000;44:852–9.
[3] Tamura T, Usui S, Murakami S, et al. Comparisons of multi b-value DWI signal analysis with pathological specimen of breast cancer. Magn Reson Med 2012;68:890–7.
[4] Le Bihan D, Breton E, Lallemand D, et al. MR imaging of intravoxel incoherent motions: application to diffusion and perfusion in neurologic disorders. Radiology 1986;161:401–7.
[5] Patel J, Sigmund EE, Rusinek H, et al. Diagnosis of cirrhosis with intravoxel incoherent motion diffusion MRI and dynamic contrast-enhanced MRI alone and in combination: preliminary experience. J Magn Reson Imaging 2010;31:589–600.
[6] Döpfert J, Lemke A, Weidner A, et al. Investigation of prostate cancer using diffusion-weighted intravoxel incoherent motion imaging. Magn Reson Imaging 2011;29:1053–8.
[7] Sumi M, Van Cauteren M, Sumi T, et al. Salivary gland tumors: use of intravoxel incoherent motion MR imaging for assessment of diffusion and perfusion for the differentiation of benign from malignant tumors. Radiology 2012;263:770–7.
[8] Rapacchi S, Wen H, Viallon M, et al. Low b-value diffusion weighted cardiac magnetic resonance imaging: initial results in humans using an optimal time-window imaging approach. Invest Radiol 2011;46:751–8.
[9] Spinner GR, von Deuster C, Tezcan KC, et al. Bayesian intravoxel incoherent motion parameter mapping in the human heart. J Cardiovasc Magn Reson 2017;19:85–98.
[10] Mou A, Zhang C, Li M, et al. Evaluation of myocardial microcirculation using intravoxel incoherent motion imaging. J Magn Reson Imaging 2017;46:1818–28.
[11] Zhang H, Xue H, Alto S, et al. Integrated shimming improves lesion detection in whole-body diffusion-weighted examinations of patients with plasma disorder at 3 T. Invest Radiol 2016;51:297–305.
[12] Cohen AD, Schieke MC, Hohenwalter MD, et al. The elfect of low b-values on the intravoxel incoherent motion derived pseudodiffusion parameter in liver. Magn Reson Med 2015;73:306–11.
[13] Abdullah OM, Gomez AD, Merchant S, et al. Orientation dependence of microcirculation-induced diffusion signal in anisotropic tissues. Magn Reson Med 2016;76:1252–62.
[14] Steidle G, Schick F. Addressing spontaneous signal voids in repetitive single-shot DWI of musculature: spatial and temporal patterns in the calves of healthy volunteers and consideration of unintended muscle activities as underlying mechanism. NMR Biomed 2015;28:801–10.
[15] Togao O, Hiwatashi A, Yamashita K, et al. Differentiation of high-grade and low-grade diffuse gliomas by intravoxel incoherent motion MR imaging. Neuro Oncol 2016;18:132–41.
[16] Du X, Zhang W, Zhang H, et al. Deep regression segmentation for cardiac bi-ventricle MR images. IEEE Access 2018;6:3828–38.
[17] Zhang H, Gao Z, Xu L, et al. A meshfree representation for cardiac medical image computing. IEEE J Transl Eng Health Med 2018;6:1–2.
[18] Zou Q, Luo C, Gong LG. Progress of diffusion-weighted imaging based on intravoxel incoherent motion in kidney diseases. Chin J Radiol 2016;50:235–7.

[19] Xie LF, Liang CH. Research progress of intravoxel incoherent motion imaging in liver. Chin J Radiol 2014;48:77–9.
[20] Deux JF, Maatouk M, Vignaud A, et al. Diffusion-weighted echo planar imaging in patients with recent myocardial infarction. Eur Radiol 2011;21:46–53.
[21] Takahara T, Kwee TC. Low b-value diffusion-weighted imaging: emerging applications in the body. J Magn Reson Imaging 2012;35:1266–73.
[22] Ji TT, Yang C, Yu CX. Application value of MRI in evaluating the effects of hypertension on cardiovascular system. J Clin Radiol 2012;31:1670–2.
[23] Laissy JP, Gaxotte V, Ironde-Laissy E, et al. Cardiac diffusion-weighted MR imaging in recent, subacute, and chronic myocardial infarction: a pilot study. J Magn Reson Imaging 2013;38:1377–87.